

文章编号:1005-9865(2010)02-0050-08

Fully nonlinear hydrodynamic simulation of submerged horizontal plate

WANG Ke, ZHANG Zhi-qiang, ZHANG Xi

(State Key Laboratory of Structural Analysis for Industrial Equipment, Dalian University of Technology, Dalian 116024, China)

Abstract: A fully nonlinear numerical wave tank technique is utilized to simulate a submerged horizontal plate. The plate is supposed to be thin, rigid and very close to free surface of water at finite depth. At each time step the wave profile is traced by fourth order Runge-Kutta method and damping zone is used to absorb outgoing wave and let simulation perform long time. Smoothing and regridding method is adopted to remove high gradients of control nodes on free surface. Numerical validities of wave tank technique are compared with linear theory of wave elevation and hydrodynamic wave interaction with a half floating cylinder, and the results show excellent agreements. Time domain wave plate simulation is carried out under the wave generated by wave maker. The free surface deformation, wave exciting force and Fourier analysis of wave plate interaction are carried out in time domain. It is found that for plate very close to free surface, strong nonlinearity occurs, which reveals the limitation of linear theory.

Key words: numerical wave tank; submerged horizontal plate; Runge-Kutta method; hydrodynamic wave interaction

CLC number: P751 **Document code:** A

水下平板与波浪相互作用完全非线性数值模拟

王 科, 张志强, 张 犀

(大连理工大学 工程力学系工业装备结构分析国家重点实验室, 辽宁 大连 116024)

摘 要: 利用完全非线性数值波浪水槽技术研究水下平板与波浪的相互作用。假定水下平板厚度极薄、刚性, 位于有限水深并且非常接近自由水面。应用四阶龙格库塔方法追踪每一时刻的波面形状, 采用阻尼层来吸收反射波以保证算法的稳定性, 同时引入平滑和重组的方法抑制自由表面控制点的较高梯度。通过对波浪与浮动圆柱相互作用的数值模拟证实了数值波浪水槽方法的有效性, 计算结果与线性理论吻合良好。在波浪数值水槽方法中引入造波板模拟波浪产生并与水下平板发生相互作用, 应用傅立叶解析方法对波面变形、波浪力作了分析。结果表明在板非常接近自由水面的情况下会表现出很强的非线性, 揭示了线性理论的局限性。

关键词: 波浪数值水槽; 水下平板; 龙格库塔法; 波浪水动力作用

The numerical wave tank method is utilized in recent decades to simulate fully nonlinear wave body interaction by boundary element method. Most of them are based on the Mixed Eulerian Lagrangian (MEL) method pioneered^[1] under the assumption of inviscid flow with irrotational motion and has been applied to several simulations of 2-D free surface flows by many researchers^[2-21].

Successful nonlinear simulation based on MEL method should solve following numerical problem: 1) wave generation and absorption to keep simulation long time; 2) numerical treatment at the interaction between the body and the free surface; 3) an accurate evaluation of the time derivative of the velocity potential, because the pressure and velocity field of

Received data: 2009-05-08

Foundation Items: Scientific Research Foundation for the Returned Overseas Scholars, State Education Ministry (2007-24)

Biography: WANG Ke (1970 -), Male, Ph. D., Ocean Engineering. E-mail: kwang@dlut.edu.cn

the flow are coupled; 4) Numerical accuracy of arbitrary shape body.

To overcome above mentioned problem, some robust and efficient methods are used in this paper: 1) A piston type wavemaker is installed at one end of wave tank to generate incident wave, a damping zone is allocated at tank ends to absorb reflection waves; 2) double node technique is used to remove singularity of integration in boundary element method, smoothing and regridding method is adopted to suppress deformation of free surface to avoid wave breaking; 3) direct calculation of time derivative of the velocity potential ϕ_t in Bernoulli's equation is chosen to make a stable solution; 4) linear element is adopted with analytic integration method to expend to complicated structure without numerical errors.

The MEL method has be compared with linear theory of wave elevation and hydrodynamic wave interaction with a half floating cylinder, the results are in excellent agreements. The objective of present study is to establish a robust and accurate method which can simulate 3-D floating body in waves, for that case to be accomplished, fully nonlinear wave tank technique is expended to simulate wave acting on a submerged horizontal plate very close to free surface, a flow configuration with special geometry. The free surface deformation, wave exciting force and Fourier analysis of wave plate interaction are carried out in time domain, it is found that for plate very close to free surface strong nonlinearity occurs, which reveals the limitation of linear theory.

Section 1,2 reviews mathematical formula of wave body interaction problem in time domain. Results and discussion are given in section 3, conclusion and remarks are given in section 4.

1 Theoretical Formulations

Assume fluid is in-viscid, incompressible and its motion is irrotational, consider a volume of water Ω , surrounded by boundaries consisting of free surface, submerged plate, tank bottom and sidewalls. A Cartesian coordinate system is chosen in the undisturbed free surface with x -axis on the water line and y -axis positive upward, the origin is on free surface of wave maker as shown in Fig.1. S_B is rigid wall denoting the far field radiation of outgoing waves; S_W is damping zone with one wavelength long; S_F is free surface, S_0 is piston type wave maker and S_H is submerged plate. The normal vector n is positive outward of the fluid.

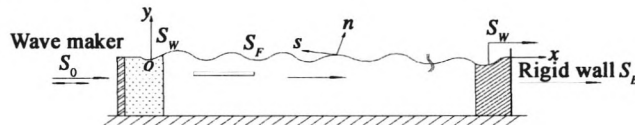


Fig. 1 Two dimensional wave tank fluid domain

Introduce similar treatments as Longuet-Higgins and Cokelet^[1]; all variables are non-dimensional in terms of fluid density ρ , gravity acceleration g , water depth H as below:

$$\begin{aligned} \rho' &= \frac{\rho}{\rho} = 1, & g' &= \frac{g}{g} = 1, & h' &= \frac{H}{H} = 1 \\ x' &= \frac{x}{H}, & y' &= \frac{y}{H}, & t' &= t \sqrt{g/H} \\ p' &= \frac{p}{\rho g H}, & F' &= \frac{F}{\rho g H^2}, & \omega' &= \omega \sqrt{H/g} \end{aligned} \tag{1}$$

where p' , F' , ω' denotes water pressure, wave force and wave circular frequency respectively. The prime, which means non-dimensional values, can be omitted from now on unless specially stressed.

With the assumption of potential flow, the fluid velocity u becomes gradient of velocity potential $\phi(x, y; t)$, the governing equation and boundary conditions for $\phi(x, y; t)$ in whole wave field can be listed as following:

$$\left\{ \begin{array}{l} \nabla^2 \phi = 0, \quad \text{in fluid domain } \Omega \\ \frac{Dx}{Dt} = \frac{\partial \phi}{\partial x} - v(x_e)(x - x_e), \quad \text{on free surface } S_F \\ \frac{Dy}{Dt} = \frac{\partial \phi}{\partial y} - v(x_e)(y - y_e), \quad \text{on free surface } S_F \\ \frac{D\phi}{Dt} = -y + \frac{1}{2}(\nabla \phi)^2 - v(x_e)(\phi - y_e), \quad \text{on free surface } S_F \\ \frac{\partial \phi}{\partial n} = 0, \quad \text{on plate } S_H \\ \frac{\partial \phi}{\partial n} = -U, \quad \text{on wave maker } S_0 \\ \frac{\partial \phi}{\partial n} = 0, \quad \text{on rigid wall } S_B \end{array} \right. \quad (2)$$

In order to get wave exciting force and moment on plate, the term $\partial \phi / \partial t$ included in wave pressure should be obtained, the normal backward finite difference method has large numerical errors and will cause numerical instability, here the method of directly calculating of $\partial \phi / \partial t$ is employed. Since $\partial \phi / \partial t$ also satisfies Laplace Equation, the boundary value problem for it can be expressed^[3,17]:

$$\left\{ \begin{array}{l} \nabla^2 \phi_t = 0, \quad \text{in fluid domain } \Omega \\ \frac{\partial \phi_t}{\partial n} = 0, \quad \text{on plate } S_H \\ \frac{\partial \phi_t}{\partial n} = 0, \quad \text{on rigid wall } S_B \\ \phi_t = -y - \frac{1}{2}(\nabla \phi)^2, \quad \text{on free surface } S_F \\ \frac{\partial \phi_t}{\partial n} = Un - U \frac{\partial \nabla \phi}{\partial n}, \quad \text{on wavemaker } S_0 \end{array} \right. \quad (3)$$

In equation(2),(3), U is velocity of wave maker, $\phi_t = \partial \phi / \partial t$. $v(x_e)$ is damping coefficient, x_e, ϕ_e denote equilibrium state values. An artificial damping technique is applied here to satisfy the radiation condition at tank ends to make the simulation perform long time. Passing through this damping zone in whatever direction of propagation, the wave will greatly lose energy^[7-8]. The wave maker has been started gradually from initial still water during early time to avoid numerical instability caused by abrupt impulse on wave field.

2 Numerical procedure

If define $\Phi = (\phi; \phi_t)$ and use Green second identity in fluid domain Ω , following boundary integral equation can be obtained:

$$C\Phi + \int_{S_B+S_0+S_H} \Phi \frac{\partial G}{\partial n} ds - \int_{S_F+S_w} G \frac{\partial \Phi}{\partial n} ds = \int_{S_B+S_0+S_H} G \frac{\partial \Phi}{\partial n} ds - \int_{S_F+S_w} \Phi \frac{\partial G}{\partial n} ds \quad (4)$$

Where Green function $G(P, Q)$ can be written as:

$$\left\{ \begin{array}{l} G(P, Q) = \log r + \log r_h \\ r = \sqrt{(x - \xi)^2 + (y - \eta)^2} \\ r_h = \sqrt{(x - \xi)^2 + (y + \eta + 2h)^2} \end{array} \right. \quad (5)$$

In Eq.(4) and (5), C is solid angle, (x, y) and (ξ, η) are field point and source point respectively. Green function $G(P, Q)$ including mirror image in water bottom, can exclude the integration on water bottom in Eq. (4) and Double point technique is set to remove the weak singularity between intersection of boundaries.

By use of linear element, the integral equation (4) can be represented in the discrete form:

$$\sum_{l=1}^{n_B} [H_{il}^{S_B}] \Phi_l + \sum_{l=n_B+1}^{n_{S_F}} [G_{il}^{S_F+S_W}] \left(\frac{\partial \Phi}{\partial n}\right)_l + \sum_{l=n_{S_F}}^n [H_{il}^{S_\rho+S_H}] \Phi_l =$$

$$\sum_{l=1}^{n_B} [G_{il}^{S_B}] \left(\frac{\partial \Phi}{\partial n}\right)_l + \sum_{l=n_B+1}^{n_{S_F}} [H_{il}^{S_F+S_W}] \Phi_l + \sum_{l=n_{S_F}}^n [G_{il}^{S_\rho+S_H}] \left(\frac{\partial \Phi}{\partial n}\right)_l \quad (i, l = 1, 2, \dots, n)$$

Where the integration on each element can be expressed as:

$$H_{il} = C(P_i) \delta_{il} + \int_{\Delta_s} N_k(\zeta) \frac{\partial G}{\partial n} ds$$

$$G_{il} = \int_{\Delta_s} N_j(\zeta) G ds \quad (i, l = 1, 2, \dots, n; k = 1, 2)$$

In Eq. (7), $N_1(\zeta)$ and $N_2(\zeta)$ are linear shape functions, $\{\phi_l, (\frac{\partial \phi}{\partial n})_l\}$ are values of l node, ζ is local coordinate in each element, δ_{il} is Delta function. Double point technique is set to remove the weak singularity between intersection of boundaries.

During wave propagation, the free surface is integrated in time using Fourth Order Runge-Kutta Method. The uniform five-point smoothing scheme like^[1] is expanded here to general five-point smoothing method^[16]. Also because of the moving of the wave maker, sometimes the phenomena that the first point on free surface over crosses the second point occurs and makes the total calculation break down. This instability can not be removed by five point smoothing scheme, since this scheme can not be accurately applied to the first or end two points. Then a new regridding method, equal-arc-length spaced method (EASM), is used to create new Lagrangian points on the free surface after each time stepping. The EASM method can also be used to equally reallocated control points clustered or with high gradient. After these artificial treatments, no saw-tooth like instability was observed and wave broken can be avoided.

3 Results and discussion

3.1 Verification of numerical wave tank model

In order to verify the efficiency of numerical wave tank technique, the wave propagation and absorption problem are investigated (Fig. 2) for an incident wave with wave period $T = 1.6$ s, wave amplitude $\eta_l = 0.04$ m, wave steepness equals 0.02, water depth $H = 2.0$ m and tank length is eight time wavelength. In numerical simulation, the total node number is 383 (40 on S_B , S_O ; 60 on S_W ; 180 on S_F) The time interval $\Delta t = T/20$ and simulating time is 20 wave periods which ensure reach of the fully steady wave state. Similarly like treatment in^[7-8], the non-dimensional parameter $\alpha = \beta = 1.0$ is chosen in damping zone without loss of efficiency.

In Fig. 2, point 103 is entrance of the damping zone at far field and point 252 denotes position one and a half wavelength from the wavemaker. Fig. 4 shows the wave elevation with time series just at point 103 before damping zone, fairly well agreement with linear theory can be observed. Fig. 5 denotes wave elevation at point 252, also excellent agreement can be attained.

To gain a further confidence of this model in wave body interaction, a half floating cylinder with forced harmonic heave motion in confined water field is calculated^[2]. The heave motion is $y(t) = A_3 \sin(\omega t)$, where A_3 is motion amplitude and ω is harmonic motion frequency. The linear restored force, $-2\rho g R y(t)$, is excluded, while R is radius of cylinder, ρ is water density and g is gravity acceleration. The calculation sketch is shown in Fig. 3. Fig. 6 shows non-dimensional comparison of hydrodynamic forces of current method and T. Vinjie's method, well agreements can be observed. Since damping zones are added on tank ends to absorb reflecting wave, the motion of cylinder can be simulated with very long time and this can be found in Fig. 7.

3.2 Wave elevations and fourier analysis

The nonlinear simulation of wave plate interactions is listed in Tab. 1, the node and element number of wave tank is the same as Fig. 2, the element number on plate is 80 and thickness of plate is 0.005 m. If assume b_1, b_2, \dots, b_m the

amplitude of m order harmonic wave, the transmitted wave coefficients of component can be defined as $T_1 = b_1/\eta_I, T_2 = b_2/\eta_I, \dots, T_m = b_m/\eta_I$, while η_I is incident wave amplitude.

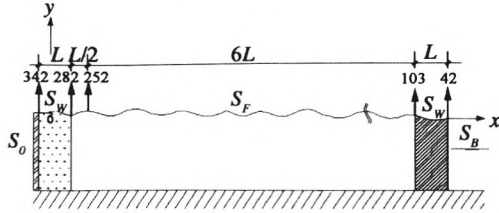


Fig. 2 Point measurements

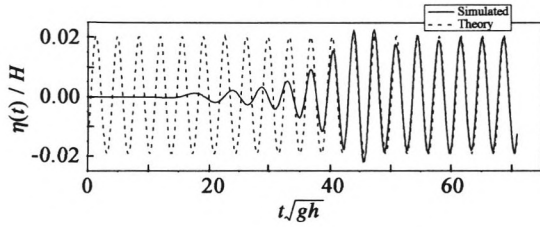


Fig. 4 Wave elevation at point 103 ($x = 5L$, not absorbed)

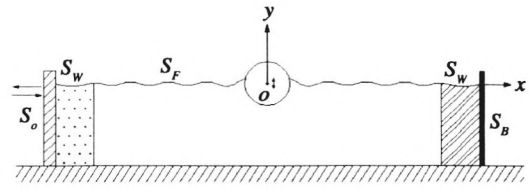


Fig. 3 Calculation sketch of half floating cylinder

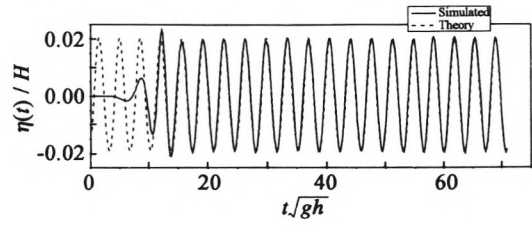


Fig. 5 Wave elevation at point 252 ($x = 1.5L$)

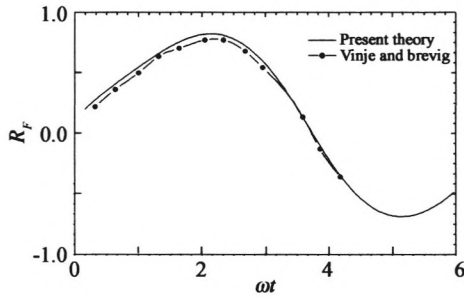


Fig. 6 Comparison of hydrodynamic force on a half-floating cylinder in forced heave motion

$$(R_F = \frac{F}{\rho g \frac{\pi}{2} R^2} (\frac{R}{A_3}), \omega \sqrt{\frac{R}{g}} = 1.0, \frac{A_3}{R} = 0.1)$$

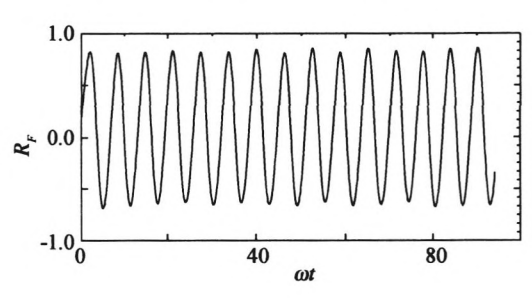


Fig. 7 Hydrodynamic force on a half-floating cylinder in forced heave motion

$$(R_F = \frac{F}{\rho g \frac{\pi}{2} R^2} (\frac{R}{A_3}), \omega \sqrt{\frac{R}{g}} = 1.0, \frac{A_3}{R} = 0.1)$$

Tab. 1 Calculations of different order wave transmitted coefficients

Wave period T/s	0.8	1.7	2.5
Wave height $(2\eta_I)/cm$	3.8	6.4	5.6
Plate submergence $(d)/m$	0.1	0.1	0.1
Plate longitude $(2a)/m$	1.2	1.2	1.2
Ratio $(d/2\eta_I)$	2.63	1.56	1.79
Ratio $(2a/L)$	1.10	0.28	0.12
Time interval (Δt)	$T/20$	$T/37$	$T/37$
First Order Transmitted coeffi. (T_1)	0.526 0	0.187 5	0.890 0
Second Order Transmitted coeffi. (T_2)	0.014 9	0.003 2	0.037 8
Third Order Transmitted coeffi. (T_3)	0.007 0	0.001 3	0.004 6

Fig.8 shows whole free surface profile for intermediate wave ($T = 1.7$ s) at five different time interval from $14T$ to $15T$. From Fig. 8, we can clearly observe the efficient wave elevation reduction before and after plate and the incident wave amplitude has been greatly eliminated. In order to further investigate this process, concentration is focused on four specific points $x_1 = 2.25L, x_2 = 2.5L, x_3 = 2.75L$ and $x_4 = 3L$ on free surface within one wave length behind plate, while L is wave length. The end of plate is at position $x = 2.27L$, and point $x_1 = 2.25L$ is just on top of plate.

The elevations of above four points with time series are listed in Fig. 9. It is found that wave elimination takes place very fast within first wave length behind plate, actually at first quarter of wave length before $x_2 = 2.5L$, the wave elimination process nearly comes to end. This drastic wave profile deformation within short time interval implies strong nonlinear fluid interaction and wave energy will be relocated within wider frequency range.

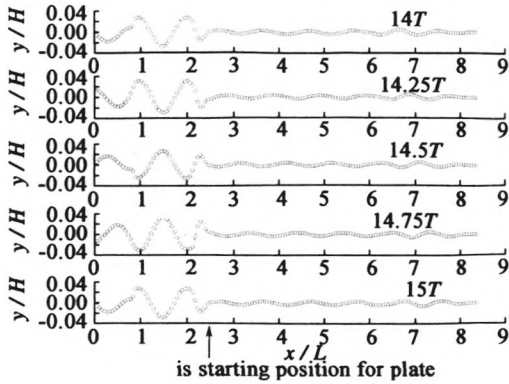


Fig. 8 Wave profile of free surface at time $14T$ to $15T$ for $T = 1.7$ s

The wave elevations at points $x = 5L$ from wave maker have been recorded in Fig. 10 for different waves. From this figure it is found that in short wave case at non-dimensional time 35, the wave elevation behind plate will reach its steady state and wave height will be reduced 50%. For intermediate wave case the wave height is reduced about 80% while only 10% wave height has been reduced for long wave case.

When wave is acting upon plate, the profile of free surface will be deformed and kinematics motion energy of free surface will be dissipated drastically and interact with fluid around plate. The conventional linear theory can not reveal this variance. This can be confirmed by following Fourier analysis in Fig. 11. From Fig. 11, it is clearly observed that at point $x_2 = 2.5L$, the wave has decomposed into high order high harmonic short waves to three order, the amplitude of second order component is about 14.3% of basic component and the amplitude of third order component is about 10% of basic component. While at far field point, $x = 5L$ the second and third order wave almost disappear, and only first order wave component exists.

From Tab. 1, it is found that at far field the first order is dominated to any kind wave. The minimum first order wave transmitted coefficient is 0.1875 for intermediate wave while relative submergence is $d/(2\eta_l) = 1.56$, and relative plate length $2a/L$ is 0.28. The wave transmitted coefficient is 0.89 for long wave, while relative submergence is $d/(2\eta_l) = 1.79$, and relative plate length $2a/L$ is 0.12. For short wave case, when relative submergence $d/(2\eta_l) = 2.63$, the wave transmitted coefficient is 0.526, larger than intermediate wave. This is because the plate is deep submerged and the effecting of $d/(2\eta_l)$ is more dominated than $2a/L$. These first order results are consist with experiments of Fig. 12^[9-10].

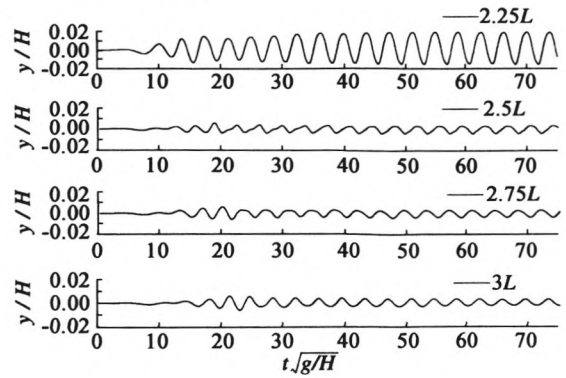


Fig. 9 Wave elevations at different positions with time series for $T = 1.7$ s

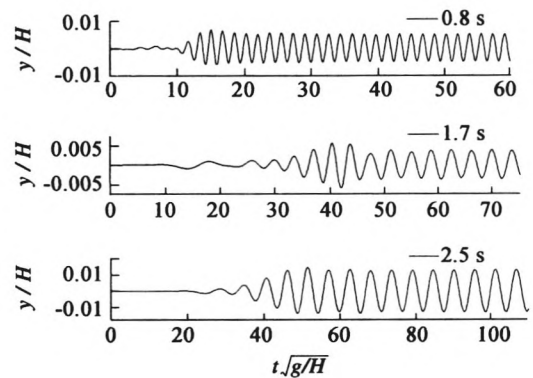


Fig. 10 Wave elevations at position $x = 5L$ with time series for different waves

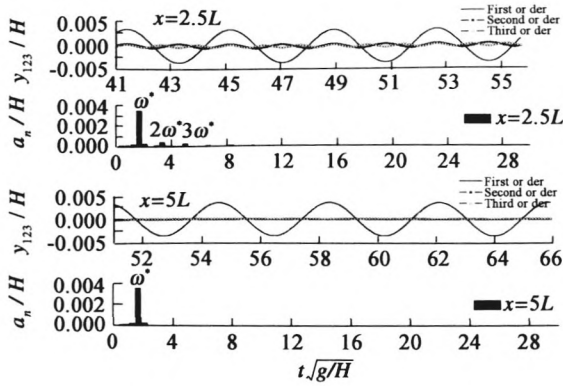


Fig. 11 Fourier and spectra analysis of transmitted wave at $x = 2.5L$ and $x = 5L$ for $T = 1.7$ s

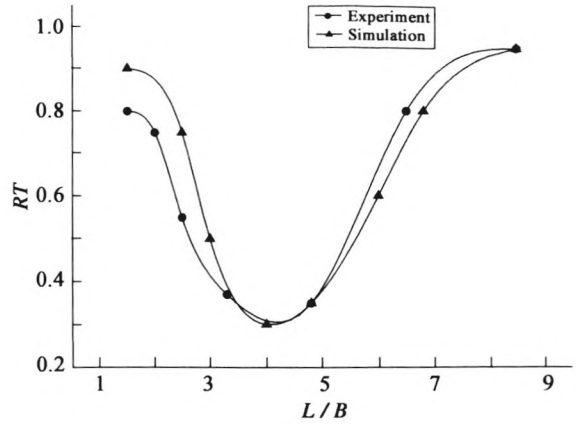


Fig. 12 Comparison results of experiment and simulation (wave amplitude $\eta_l = 3$ cm, submergence $d = 7.5$ cm)

3.3 Wave exciting force and fourier analysis

Omitting effecting of hydrostatic force, the wave exciting force of short wave ($T = 0.8$ s) with time series are shown in Fig. 13, the curves for vertical and moment of wave exciting force are nearly symmetric around x axis while the occurrence of narrower crest of horizontal force means stronger nonlinear effecting with plate.

Fig. 14 and Fig. 15 give wave exciting force with time series for intermediate wave ($T = 1.7$ s) and long wave ($T = 2.5$ s) respectively. Comparing with short wave, double spikes occur near positive crest of horizontal, vertical and moment of intermediate wave. For long wave case (Fig. 15), double spikes exist in both crest and trough of horizontal force, while the vertical force moves around, $F_y/\rho g H^2 = -0.02$ which means during the process of long wave interacting with plate, there is a constant drift force acting on plate.

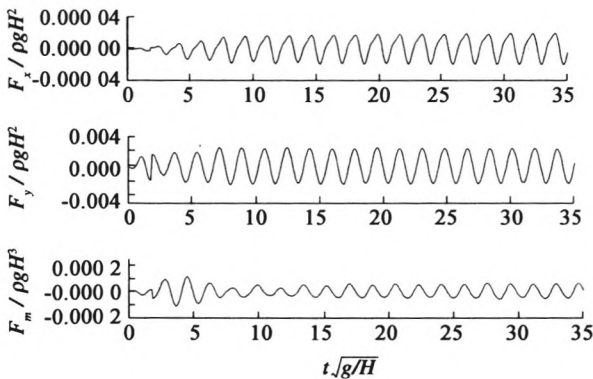


Fig. 13 Wave force and moment for $T = 0.8$ s with time series

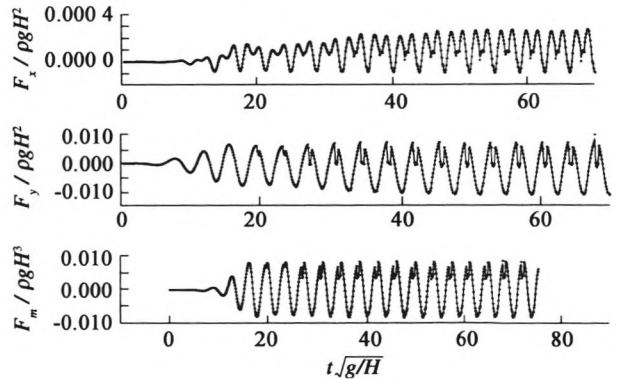


Fig. 14 Wave force and moment for $T = 1.7$ s with time series

The Fourier analysis of wave exciting force will be carried out only for very effective intermediate wave since the non-linearity is obvious. And also because the plate is very thin and the horizontal force is extremely small, the discussion is ignored either. The Fourier analysis of first three order component of vertical force and exciting moment are listed in Fig. 15, In (a), (b) of Fig. 16, the basic frequency component is dominated but second order component and third order component are nearly 30% and 25% of basic component and can not be omitted. From (c) in Fig. 16, we can find that for vertical force, higher order components larger than third order are still very effective, in fact the fifth order component is about 10% of basic component.

During whole simulation, the big problem exists to express the occurring double spikes around crest of force for example in Fig. 14. The numerical errors in calculating ϕ or $\nabla \phi \cdot \nabla \phi$ for this very thin plate might be one reason, this can be observed from sharp changing of force near crest. The limitation of potential flow near the singular corner of plate might be the other reason. Future mathematical model or robust numerical algorithm should be developed to implement this conclusion.

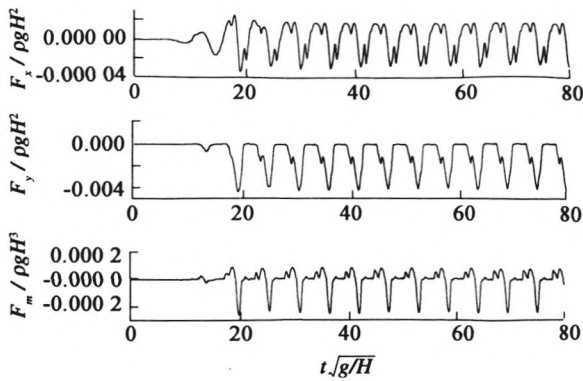


Fig. 15 Wave force and moment for $T = 2.5$ s with time series

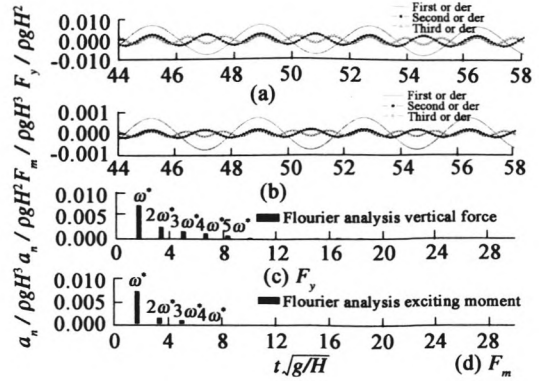


Fig. 16 Fourier (a, b) and spectra (c, d) analysis of wave force and moment for $T = 1.7$ s

4 Conclusion and remarks

A submerged horizontal plate has assumed rigid, thin and is located very close to free surface. A wave tank technique has been developed by use of boundary element method to investigate fully nonlinear wave plate interaction. In this simulation, the time stepping free surface is integrated by Fourth Order Runge Kutta Method and open boundary condition was treated by the scheme of absorbing damping zone. Smoothing and regridding algorithm are utilized to suppress free surface deformations. Different from linear solution or second order perturbation method in frequency domain, through Fourier analysis, any order wave elevation and force component can be achieved which is quite simple in mathematical treatment comparing with frequency domain problem. For a plate very close to free surface, very strong nonlinearity will occur especially in short and intermediate incident wave and this reveals the limitation of linear theory.

References:

- [1] Longuet-Higgins M S, Cokelet E. The deformation of steep surface waves on water[J]. Proc. Roy. Soc. Ser. A350, 1976:1 – 26.
- [2] Vinje T, Brevig P. Nonlinear ship motions[C]//Proc. of the 3rd. Int. Conf. on Numerical Ship Hydro. 1981:IV3-1-IV3-10.
- [3] Wu G X, Eatock Taylor R. Transient motion of a floating body in steep waves[C]//11th Int Workshop on Water Waves and Floating Bodies. Hamburg:[s. n.], 1996.
- [4] Clement. Coupling of two absorbing boundary conditions for 2D time-domain simulations of free surface gravity waves[J]. Journal of Computational Physics, 1996, 126: 139 – 151.
- [5] S Y Boo, C H Kim. Simulation of fully nonlinear irregular waves in a 3D numerical wave[C]//Proceeding of the Seventh International Offshore and Polar Engineering Conference. Osaka:[s. n.], 1994.
- [6] S Y Boo, C H Kim. Nonlinear irregular waves and forces on truncated vertical cylinder in a numerical wave tank[C]//Proceeding of the Seventh International Offshore and Polar Engineering Conference. Honolulu:[s. n.], 1997.
- [7] Tanizawa K. A nonlinear simulation method of 3D body motions in waves[J]. J. Soc. Nav. Arch. Japan, 1995, 178: 179 – 191.
- [8] Tanizawa K. Long time fully nonlinear simulation of floating body motions with artificial damping zone[J]. Journal of SNAJ, 1996, 180: 311 – 319.
- [9] Ke Wang. Study on Horizontal Plate Type Breakwater[D]. Dalian: Dalian University of Technology, 2001. (in Chinese)
- [10] Ke wang, Haigui Kang. An efficient computation method for wave tank technique[J]. Acta Oceanologica Sinica, 2001, 20: 281 – 297.
- [11] Yongxue Wang, Guoyu Wang, Guangwei Li. Experimental study on the performance of the multiple-layer breakwater[J]. Ocean Engineering, 2006, 33: 1829 – 1839, 1313.
- [12] Jepsen Skourup, Hemming A Schaeffer. Wave generation and active absorption in a numerical wave flume[C]//Proceeding of the Seventh International Offshore and Polar Engineering Conference. Honolulu:[s. n.], 1997: 85 – 91.
- [13] Yuming liu, Douglas Dommermuth, Dick K P Yue. A high order spectral method for nonlinear wave-body interactions[J]. J. Fluid Mech, 1992, 245: 115 – 136.

提高计算精度,使得 SCR 的分析更加符合工程实际。

参考文献:

- [1] Egil Giertsen, Richard Verley, Knut Schroder. Carisima a catenary riser/soil interaction model for global riser analysis[C]//Proceedings of the Interaction Conference on Offshore Mechanics and Arctic Engineering. Vancouver, Canada: American Society of Mechanical Engineers, 2004: 633 - 640.
- [2] Jun Hwah You. Numerical Model for Steel Catenary Riser on Seafloor Support[D]. Texas: Texas A&M University, 2005.
- [3] 傅俊杰, 杨和振. 深海钢悬链线立管触地点动力响应分析[J]. 海洋工程, 2009, 27(2): 36 - 40.
- [4] 畅元江, 陈国明, 许亮斌, 等. 深水管中管钢悬链线立管的非线性动力分析[J]. 中国造船, 2007, 48(增刊): 467 - 473.
- [5] Charles P Aubeny, Giovanna Biscontin, Jun Zhang. Seafloor Interaction with Steel Catenary Risers[D]. Texas: Texas A&M University, 2006.
- [6] 杜金新, Low Y M. 海洋立管 - 海床土体接触作用数值分析[J]. 工程地质计算机应用, 2008(4): 1 - 6.
- [7] 郭海燕, 高秦岭, 王小东. 钢悬链线立管与海床土体接触问题的 ANSYS 有限元分析[J]. 中国海洋大学学报, 2009, 39(3): 521 - 525.
- [8] Garrett D L. Dynamic analysis of slender rods[J]. Journal of Energy Resources Technology, 1982, 104: 302 - 307.
- [9] XiaoHong Chen. Studies on Dynamic Interaction Between Deep-water Floating Structures and Their Mooring/Tendon System[D]. Texas: Texas A&M University, 2002.
- [10] 董艳秋. 深海采油平台波浪载荷及响应[M]. 天津: 天津大学出版社, 2005: 192 - 202.
- [11] 郭斌, 唐文勇, 张圣坤. Truss Spar 平台桁架的疲劳分析方法[J]. 中国海洋平台, 2006, 21(4): 36 - 41.
- [12] 2H Offshore Engineering Ltd. Pull-out Resistance of a Pipe in a Clay Soil[R]. Report No. 1500-RPT-006, Rev 02, 2002.
- [13] Christopher Bridge, Neil Willis. Steel catenary risers-results and conclusions from large scale simulations of seabed interaction[C]//14th Annual Conference Deep Offshore Technology. 2002.
- [14] 竺艳蓉. 海洋工程波浪力学[M]. 天津: 天津大学出版社, 1991.

(上接第 57 页)

- [14] Douglas Dommermuth, Dick K P Yue. A high order spectral method for the study of nonlinear gravity waves[J]. J. Fluid Mech, 1987, 184: 267 - 288.
- [15] D G Dommermuth, D K P Yue. Numerical simulation of nonlinear axisymmetric flows with a free surface[J]. Journal of Fluid Mechanics, 1987: 178.
- [16] Pei Wang, Yitao Yao, Marshall P Tulin. An efficient numerical tank for non-linear water waves, based on the multi-subdomain approach with BEM[J]. International Journal for Numerical Methods in Fluids, 1995, 20: 1315 - 1336.
- [17] Wu G X, Ma Q W, Eatock Taylor R. Numerical simulation of sloshing waves in a 3D tank based on a finite element method[J]. Appl. Ocean Res, 1998, 20: 337 - 355.
- [18] G X Wu, R Eatock Taylor. The coupled finite element and boundary element analysis of nonlinear interactions between waves and bodies[J]. Ocean Engineering, 2000, 30: 387 - 400.
- [19] Wang C Z, Wu G X. An unstructured mesh based finite element simulation of wave interactions with non-wall-sided bodies[J]. J. Fluids & Structures, 2006, 22: 441 - 461.
- [20] Wang C Z, Wu G X. Time domain analysis of second order wave diffraction by an array of vertical cylinders[J]. J. Fluids & Structures, 2007, 23: 605 - 631.
- [21] Wang C Z, Wu G X, Drake K. Interactions between nonlinear water waves and non-wall-sided 3D structures[J]. Ocean Engineering, 2007, 34: 1182 - 1196.